Vol. 8, No. 6, December 2024, pp. 650-658

Current Optics and Photonics

Regular Paper

Single-shot Transport-of-intensity Equation Using a Lateral-displacement-beam-splitter Module for Biological Samples

Joseph Vermont Bunyi Bandoy, Cuong Manh Nguyen, An Nazmus Sakib, Suhyeon Kim, and Hyuk-Sang Kwon*

Department of Biomedical Science and Engineering, Gwangju Institute of Science and Technology, Gwangju 61005, Korea

(Received June 26, 2024 : revised September 14, 2024 : accepted September 20, 2024)

Methods using the single-shot transport-of-intensity equation (ssTIE) commonly require capturing multiple intensities in one plane. In this work, the introduction of a lateral-displacement-beam-splitter module provides another solution for ssTIE. This technique eliminates the need for multiple acquisitions at different focal positions, thereby accelerating the imaging process and avoiding mechanical translation. For implementation, the module is placed after a bright-field microscope. After implementation, we validated the system by applying it to the imaging of mammalian nerve fibers and red blood cells. This approach holds promise for biological and medical research.

Keywords : Biomedical optics, Microscopy, Transport of intensity equation
OCIS codes : (120.5050) Phase measurement; (170.170) Medical optics and biotechnology; (180.0180) Microscopy; (230.1360) Beam splitters

I. INTRODUCTION

The transport-of-intensity equation (TIE) is a deterministic, noninterferometric quantitative phase imaging (QPI) technique that relies on obtaining multiple defocused images for phase measurement. It was first derived with Green's function as a solution to phase retrieval [1]. Other solutions in deriving this equation have been explored using the Poynting vector [2], using Zernike- and fast Fourier transform (FFT)-based solutions [3, 4], until the generalized TIE in phase-space solution [5]. With its versatility, the application of this technique ranges from optical microscopy [6] to X-ray imaging [7] and diffraction tomography [8].

Implementation of TIE requires defocusing. A standard procedure for data acquisition is by manual translation of the stage to achieve defocusing, then obtaining two defocused images and one focused. This can be implemented with a common bright-field microscope, where three images are recorded [9]. Such work has also led to the customization of the microscope to perform automated defocus [10]. While the standard procedure for this technique requires three images, using just two images is also possible. On the other hand, the FFT-based solution requires only two images: One defocused and one focused images [11]. This solution enables the use of stacks of images that are evenly spaced and higher orders for the TIE. Multiple stacks of images taken from different positions can be utilize for phase measurements [12]. However, acquiring three images is time-consuming, which may be a challenge for real-time imaging. Also, considering the higher orders for multiple images may be computationally expensive.

These challenges have led to research that solves the translation problem. With this, single-shot methods have been presented; This technique mainly captures multiple planes in one camera, which is more efficient and can be practical. In 2010, the first attempt at the single-shot

*Corresponding author: hyuksang@gist.ac.kr, ORCID 0000-0002-3387-210X

Color versions of one or more of the figures in this paper are available online.

pISSN: 2508-7266 / eISSN: 2508-7274 https://doi.org/10.3807/COPP.2024.8.6.650

transport of intensity equation (ssTIE) method was demonstrated. In this attempt, the quantitative-phase methodology was employed in a volume-holographic microscope. This technique produces laterally separated images coming from different focal planes due to the volume hologram, and the resulting images are used for phase recovery using the TIE. Furthermore, five multiplexed images may be produced with gratings in one hologram [13].

The main goal of implementing ssTIE is to capture multiple images from different axial locations at once, avoiding the mechanical or electrical translations of the conventional TIE. From here, various ssTIE methods have been implemented. A system can be built with a common bright-field microscope with a module that is Michelson-based in configuration, using a mirror and a spatial light modulator (SLM) in its paths [14], or with a retroreflective mirror to produce two images that are flipped relative to each other [15]. Moreover, a simplified version of the Michelson-based technique has been implemented using two mirrors, where one of the mirrors is tilted to generate laterally separated beams [16]. On the other hand, this technique has also been implemented by phase-mask encoding, and by designing a diffractive optical element to split the beams. First, multifocal planes can be captured all together for real-time QPI, as a result of programming a phase-mask encoded in the SLM [17]. In a method for doing so, Greek-ladder sieves were designed to simultaneously produce biplanar images at a single recording plane [18]. Similarly, a diffractive optical element placed on the Fourier plane of the sample to produce two defocused intensity distributions using polarization multiplexing was reported [19]. These various ssTIE methods have advanced the capabilities of QPI, offering efficiency in image acquisition from different planes simultaneously. However, SLM is known to be expensive because of its technology, and designing optical elements may be complicated.

Our proposed method offers a novel approach to single-shot QPI by utilizing a lateral-displacement beam splitter (LDBS) to capture displaced images with different focal planes simultaneously. This method eliminates the need for multiple measurements that require manual translation, as is necessary in conventional TIE techniques. By avoiding manual translation, this approach simplifies data acquisition and reduces the effort needed for imaging. As a result, the overall imaging process becomes more efficient. Our findings demonstrate the efficacy of this approach in both quantitative phase targets and biological samples, highlighting its potential for faster QPI.

II. THEORY AND METHODOLOGY

2.1. Transport-of-intensity Equation

The TIE can be derived using the Poynting theorem, which is the conservation of energy in electromagnetics. By definition, the Poynting vector **S** represents the directional energy flux of an electromagnetic field, described by this closed integral,

$$\oint \langle \mathbf{S} \rangle ds = 0, \tag{1}$$

where the expression in differential form is the divergence of its time average,

$$\nabla \cdot \langle \mathbf{S} \rangle = 0. \tag{2}$$

The time-averaged Poynting vector is related to the intensity of flux density and the gradient of the phase,

$$\langle \mathbf{S} \rangle = \frac{1}{k} I(x,z) \nabla \emptyset(x,z), \tag{3}$$

where I is the intensity, ∇ denotes the del operator representing the lateral gradient in the x- and y-directions, and ϕ is the phase. When the expression is decomposed into transverse and longitudinal components, it becomes

$$-k \frac{\partial I(x,z)}{\partial z} = \nabla \cdot [I(x,z) \nabla \emptyset(x)]. \tag{4}$$

Here the left-hand side of the equation is the axial intensity's derivative, and the other side is the transverse energy. Solving for the phase gives us its relationship to the intensity,

$$\varphi = -F^{-1}\left\{k^{-2} F\left\{\nabla \cdot \left[I^{-1} \cdot \nabla\left(F^{-1}\left(k^2 F\left(\frac{\partial}{\partial z} I\right)\right)\right)\right]\right\}\right\}. \tag{5}$$

The phase-retrieval method is a Fourier-transform-based solution that is used for the intensities. Furthermore, the intensities as a function of position are the defocused $I(x, y, -z)$, focused $I(x, y, z)$, and average $I(x, y, z_0)$. Two beams are observed for lateral separation. The intensity of the of the two images can be used to compute the focused image by approximately averaging them [20]. Thus,

$$I(x,y,z_0) = \frac{I(x,y,z)+I(x,y,-z)}{2}, \tag{6}$$

and

$$\frac{\partial I}{\partial z} = k \frac{I(x,y,z)-I(x,y,-z)}{2\Delta z}. \tag{7}$$

The intensity derivative is computed by taking the difference between two recorded images, which are then taken at different positions along the optical axis. This difference is then divided by the distance separating the two images. The average and the intensity derivative are then used to compute the phase.

2.2. Conventional Transport-of-intensity Equation

The conventional TIE method requires three images: One focused, one overfocused, and one under focused [9–11]. This work follows Eqs. (6) and (7), where the focused

and one overfocused image are needed. To implement this experimentally, manual translation is used via a precision linear stage (XR25; Thorlabs, NJ, USA) for the camera mount. The stage allows for a minimum translation of 10 μm. This setup enables the acquisition of the focused and defocused images necessary for phase reconstruction, by moving the sample along the optical axis.

2.3. Quantitative Phase Target

The quantitative phase target (Benchmark Technologies, MA, USA), characterized by a nominal height of 350 nm and an estimated height of 374.3 nm according to the manufacturer, serves as a resolution target for QPI in this study. The phase values are calculated with the following expression,

$$\varphi = \frac{2\pi\Delta n}{\lambda} t, \tag{8}$$

where Δn is the difference between the index of refraction of air and the index of refraction of medium, λ is the wavelength of the incident light, and t is the height of the target. According to the manufacturer, the refractive index of the target material is 1.52. Following the equation yields a nominal phase value of 2.19 radians and an estimated phase value of 2.34 radians.

2.4. Lateral-displacement Beam Splitter

For the controlled defocus, a LDBS is used. In Fig. 1, the sides of the right-triangle part of LDBS are 10 mm long. The main function of the LDBS is to split the incident beam into two displaced parallel beams. When the beam is inside the LDBS, the propagation of the incident beam normal to the surface impinges the hypotenuse of the triangular component of the LDBS, eventually exiting the interface. Meanwhile, the second beam propagates along the rhomboid part and is reflected until it emerges parallel to the first beam. The second beam propagates 10 mm farther than the first beam.

2.5. Experimental Setup

An LED is used as a light source, with an aspheric condenser lens attached for illumination and collimation. A green bandpass filter is also attached to the LED. This is followed by a field iris, field lens of 150-mm focal length, and aperture iris. The field iris is used for light-intensity adjustment, while the aperture iris limits the size of the beam diameter. The two irises are placed 150 mm before and after the lens. The light is then focused by a lens with a focal length of 30 mm. The light is focused where the sample is placed, with an objective lens having 10× magnification followed by a tube lens for collimation. Here the lateral-displacement beam splitter is placed to create two laterally separated beams that are followed by an optical glass plate and then recorded using a camera, as shown in Fig. 2.

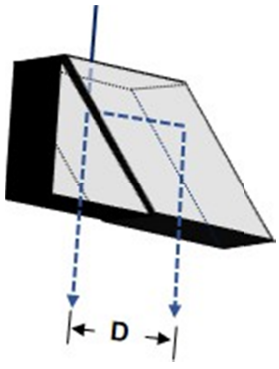

FIG. 1. A lateral-displacement beam splitter (LDBS) for controlled defocus, with D as the beam separation.

III. RESULTS AND DISCUSSION

In this study, 10-mm and 20-mm LDBSs are characterized to assess their effectiveness and phase reconstruction. The LDBS is selected for this study due to its original application in holography, where it was used to separate the reference and object beams [21]. This capability of precise beam separation has inspired its implementation in the TIE setup, allowing for effective distinction between the focused and defocused beams that are necessary for accurate phase reconstruction.

Digital alignment of the images captured from the microscope is achieved by selecting a reference point on the resolution target and identifying its corresponding point with the duplicated beam. These matched coordinates are used to accurately align the images, ensuring precise image processing and phase reconstruction.

3.1. Imaging with a 10-mm Lateral-displacement Beam Splitter

A 10-mm visible nonpolarized LDBS is used to achieve lateral separation between images. For this setup, a microscope objective lens (60×/0.85; Newport Co., CA, USA) and charge-coupled device (CCD) camera (Thorlabs 8051; Thorlabs) are used. An image is captured to check the microscope's ability to achieve separation with defocus, as shown in Figs. 3(a) and 3(b), which confirm the focused and defocused states resulting from the use of the LDBS. Then, the quantitative-phase target's grating area with a nominal height of 350 nm is used to validate the micro-

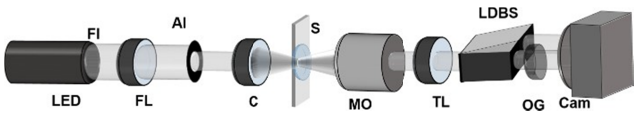

FIG. 2. Experimental setup: A light-emitting diode (LED) is filtered with an attached green bandpass filter and field iris (FI). A field lens (FL) follows, with an aperture iris (AI) and a condenser (C), for illuminating the sample (S). The sample is magnified by a microscope objective lens (MO) collimated by a tube lens (TL). The lateral-displacement beam splitter (LDBS) and optical glass plate (OG) are placed after the bright-field microscope, with a camera.

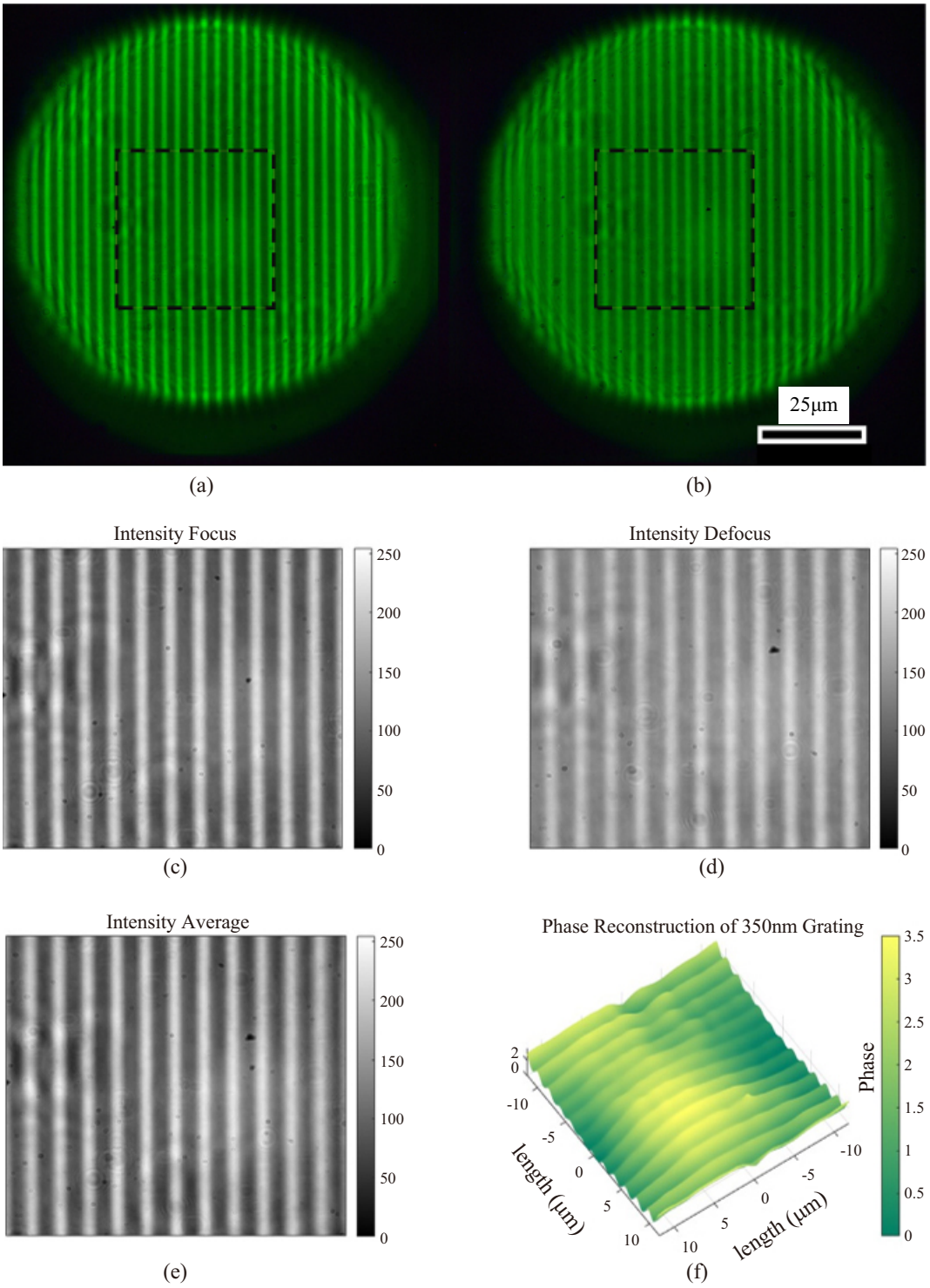

FIG. 3. Laterally separated beams captured using a 10-mm LDBS, where the (a) focused and (b) defocused beams can be observed. Scale bar: 25 μm. The dashed lines show the cropped areas of the (c) focused and (d) defocused images, and the intensity the average is shown in (e). (f) The phase reconstruction of the 350-nm grating from the quantitative phase target.

scope's performance. The cropped areas shown in Figs. 3(c) and 3(d) are used to compute the phase. Figure 3(e) shows the intensity average of the target, providing additional context for phase computation. Hence, the target provides a structure that allows us to assess the microscope's ability to reconstruct its phase information, as shown in Fig. 3(f).

3.1.1. Imaging Red Blood Cells

The microscope is next applied to biological imaging, specifically red blood cells (RBCs), to assess its perfor-

mance in biomedical applications. A human-blood-smear (Readi-Stain® human blood film slide 313152; Carolina Biological Supply Co., NC, USA) slide is used as a sample. Captured images are pegged to have dimensions of 145 × 145 pixels. The images are captured, and a single RBC is specifically selected for processing. Figure 4 shows the initial results for both techniques.

As shown in Figs. 5(a) and 5(b), the phase is calculated and the thickness is subsequently computed from Eq. 8. Next, the line profile is plotted [Fig. 5(c)].

A comparison of the proposed method to the conventional TIE method is conducted using the line profile for the RBC. In this profile, the ssTIE method (red curve) captures more pronounced features, compared to the conventional TIE method (black curve). This suggests that the proposed method captures more detailed variation in the RBC's surface profile. Moreover, the method appears to offer slightly more detail in capturing the RBC's height variations, showing higher peaks and deeper valleys, which suggests that it may provide better sensitivity to subtle surface features of the RBC. On the other hand, the conventional TIE appears to have a smoother profile.

Both methods are consistent in terms of the overall shape and position of the features, indicating that they both accurately reflect the RBC's basic structure, but the single-shot TIE shows a higher degree of detail. The comparison

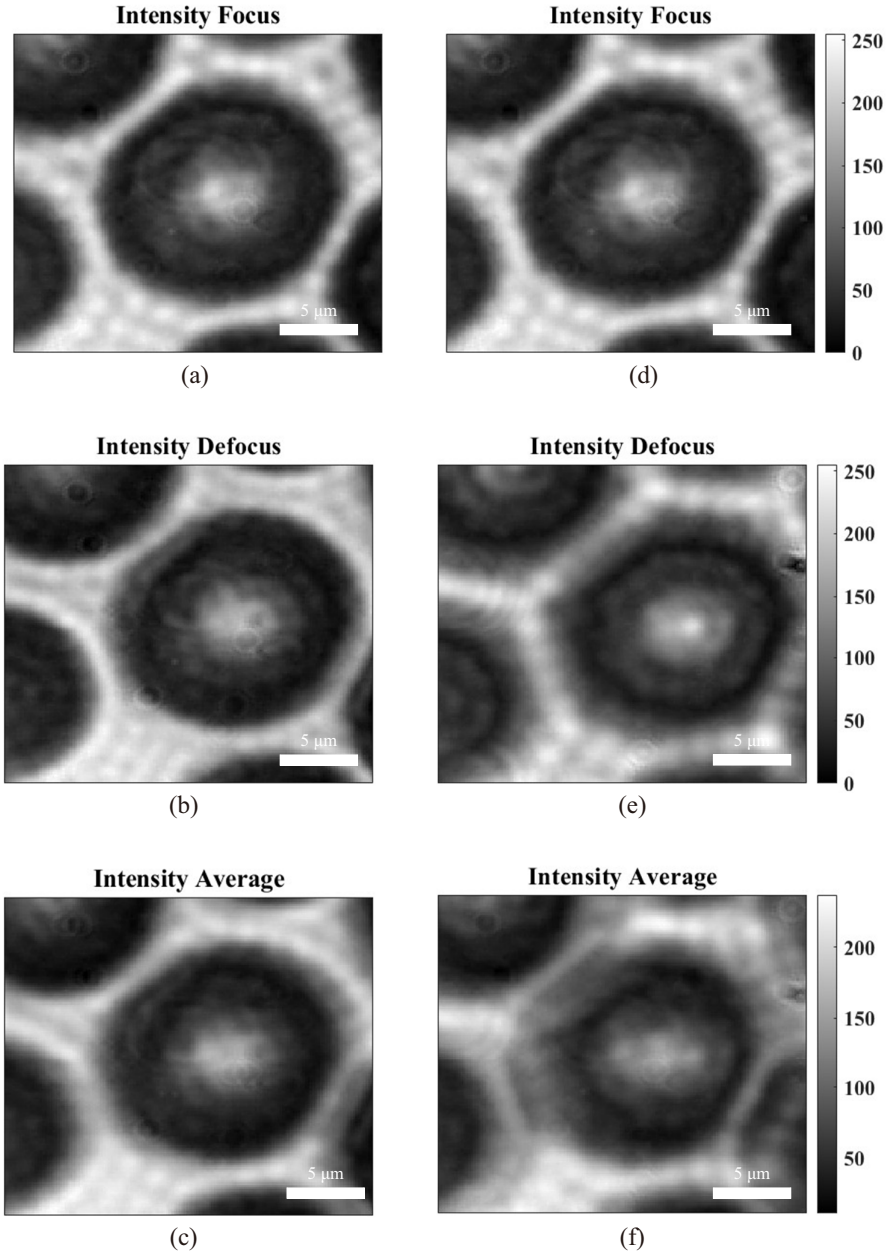

FIG. 4. Red-blood-cell intensities recorded using (a)–(c) single-shot transport-of-intensity equation (TIE) and (d)–(f) the conventional method. Scale bar: 5 μm.

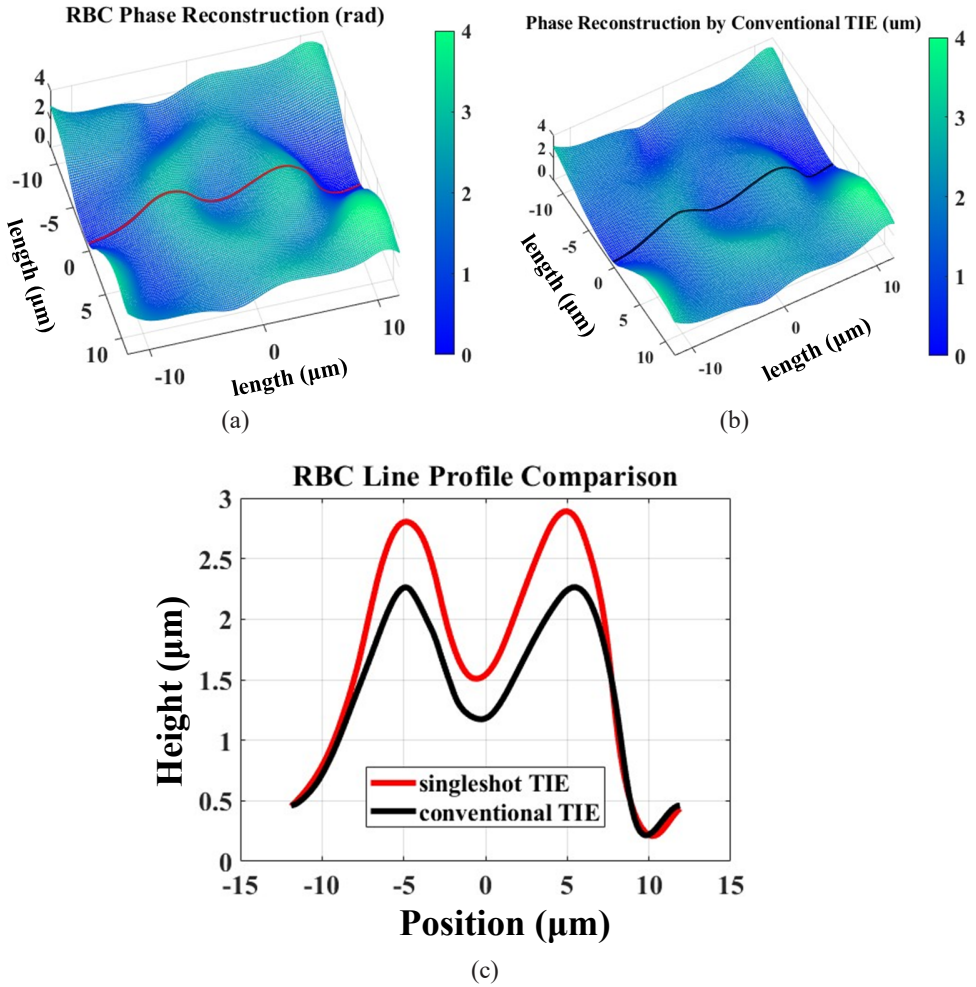

FIG. 5. Phase retrieved by (a) the single-shot method and (b) the conventional method, and (c) a line profile comparing the two methods.

suggests that while both methods are reliable, the proposed single-shot TIE may offer a more precise reconstruction of the RBC's surface.

The resulting images show that the proposed method can be used for phase reconstruction, which has strong potential in practical diagnostic applications in fields requiring phase information. The performance of the LDBS proves its capabilities in the single-shot method, as multiplane beams can be captured simultaneously, making it more efficient in data acquisition and providing another solution for the ssTIE method.

3.2. Imaging with a 20-mm Lateral-displacement Beam Splitter

In this section, a 20-mm LDBS is used to achieve lateral separation between images. For this setup, an objective lens (10×/0.3; Olympus Co., Tokyo, Japan) and camera (A7 III ILCE-7M3; Sony Group Co., Tokyo, Japan) are used.

Figure 6 shows two images that are laterally separated by 20 mm. The original setup makes use of a CCD camera with an imaging area of 18.13 mm × 13.60 mm, which makes it impossible to images both beams. For this reason, a camera with 35.6-mm sensor length is chosen to accommodate the beams. Upon image capture, the camera is controlled remotely instead of pressing the shutter trigger, to avoid misalignment. The beams are measured to be 3,445 pixels apart horizontally and 17 pixels vertically from each other. These coordinates serve as the reference for locating

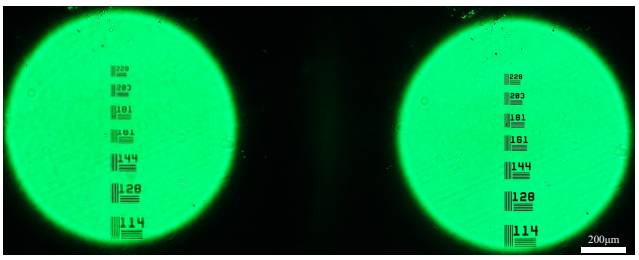

FIG. 6. Initial results for the system: Two laterally shifted beams as a result of using a lateral displacement beam splitter. The left beam is defocused, and the right beam is focused. Scale bar: 200 μm.

the specific point of the resolution target of the duplicated beam, and for reconstruction.

The NBS 1963A resolution target (Thorlabs) is used to ensure accurate scaling. Initially the quantitative-phase target was used for this purpose, but the defocus is too great, making the resolution target in the defocused beam difficult to observe.

3.2.1. Imaging Mammalian Nerve Fiber

Initially the goal was to image RBCs using the 20-mm LDBS. However, during the imaging process it is observed that the duplicated beam defocuses excessively, making it unsuitable for phase reconstruction. As a result, mammalian nerve fibers are selected for imaging, as larger structure provides a more suitable sample for this setup.

A mammalian-nerve-fiber slide (Mammal Giant Multipolar Neurons Slide, Smear, Luxol® Fast Blue #313570; Carolina Biological Supply Co.) is used as an initial sample for phase reconstruction. By using the 20-mm LDBS with mammalian nerve fibers, we are able to effectively capture both the focused and defocused beams, as shown in Figs. 7(a) and 7(b). On the other hand, for the conventional

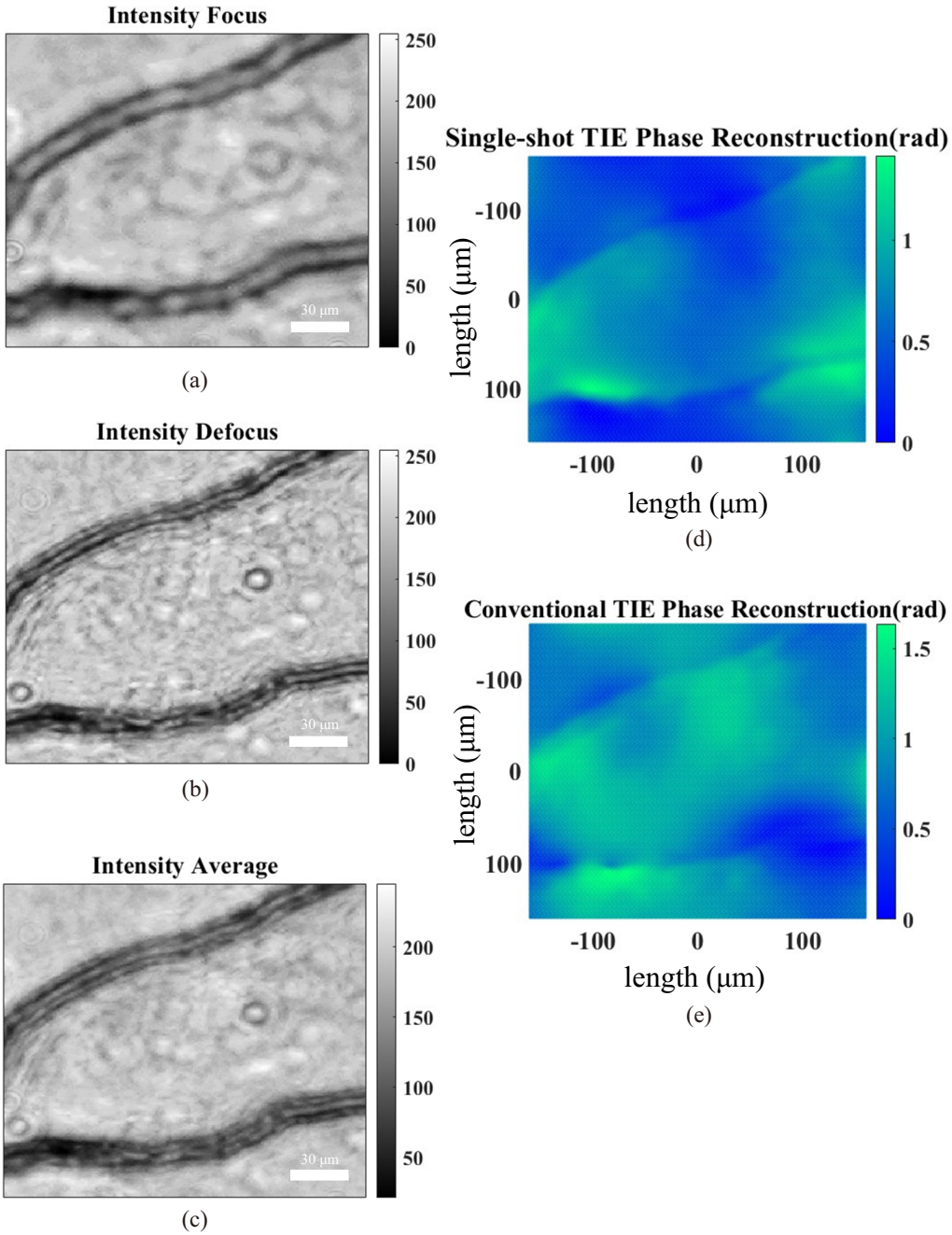

FIG. 7. Captured images of (a) focus and (b) defocus intensities, and (c) intensity average, using the single-shot method. Scale bar: 30 μm. (d), (e) Phase reconstruction of mammalian neuronal fiber from the two methods.

method in this setup, translation is performed to 20 μm to achieve defocus. Figure 7(c) displays the intensity average of the target, which provides context for phase reconstruction. For phase reconstruction the data initially range up to 104 radians, but are simplified to the range 0–2π radians, as seen in Figs. 7(d) and 7(e). In comparison, both images show a similar spatial structure or pattern of phase distribution. Though both images capture variations in the same region, the conventional method appears to be noisier, suggesting that it may be more sensitive to phase variations, but at the cost of introducing noise.

The results show that sample selection is important when choosing the LDBS beam separation. This tells us that while a 20-mm LDBS may not be ideal for samples like RBCs, imaging is possible for larger samples like mammalian nerve fibers.

While the ssTIE method using LDBS module demonstrates promising results for fast and efficient QPI, it does have some limitations. One key issue is the need for precise digital alignment of the two images, as even small misalignments can reduce accuracy. Additionally, the camera's sensor may not always fully capture both beams, as in the case of using the 20-mm LDBS, meaning the correct sensor must be chosen for each setup. Future improvements should focus on enhancing image alignment and exploring other beam-splitting techniques.

IV. CONCLUSION

This research aimed to implement a ssTIE technique for QPI. This was achieved using a common bright-field microscope. The ssTIE method was implemented using a LDBS that produced two laterally separated beams. The longer path leading to the hypotenuse of the LDBS was thought to produce a defocus, which was observed. The technique has shown its capability as another solution for ssTIE imaging. The method is advantageous in this case, as it reduces the data-acquisition time, making it more efficient.

As for any other use of controlled defocus, this method is limited in its application. This means that sample selection is important for the beam-splitter configuration. The 10-mm LDBS is suitable for imaging RBCs but not for nerve fibers, while the 20-mm LDBS works well with nerve fibers but is not ideal for RBCs.

To further understand the study, exploring alternative beam-splitting methods, such as using smaller or adjustable lateral LDBSs, could offer better control over defocus and improve the imaging performance for a wide range of biological samples.

FUNDING

This work was supported by the National Research Foundation of Korea (NRF) grant funded by the Korean government (MSIT) (Grant No. RS-2023-00302281).

DISCLOSURES

The authors declare that there are no conflicts of interest related to this article.

DATA AVAILABILITY

Data underlying the results presented in this paper are not publicly available at this time, but may be obtained from the authors upon reasonable request

REFERENCES

1. M. R. Teague, "Irradiance moments: Their propagation and use for unique retrieval of phase," J. Opt. Soc. Am. **72**, 1199–1209 (1982).
2. D. Paganin and K. A. Nugent, "Noninterferometric phase imaging with partially coherent light," Phys. Rev. Lett. **80**, 2586 (1998).
3. T. E. Gureyev, A. Roberts, and K. A. Nugent, "Phase retrieval with the transport-of-intensity equation: Matrix solution with use of Zernike polynomials," J. Opt. Soc. Am. A **12**, 1932–1941 (1995).
4. T. E. Gureyev and K. A. Nugent, "Rapid quantitative phase imaging using the transport of intensity equation," Opt. Commun. **133**, 339–346 (1997).
5. C. Zuo, Q. Chen, L. Tian, L. Waller, and A. Asundi, "Transport of intensity phase retrieval and computational imaging for partially coherent fields: The phase space perspective," Opt. Lasers Eng. **71**, 20–32 (2015).
6. N. Streibl, "Phase imaging by the transport equation of intensity," Opt. Commun. **49**, 6–10 (1984).
7. A. Snigirev, I. Snigireva, V. Kohn, S. Kuznetsov, and I. Schelokov, "On the possibilities of X-ray phase contrast microimaging by coherent high-energy synchrotron radiation," Rev. Sci. Instrum. **66**, 5486–5492 (1995).
8. C. Zuo, J. Sun, J. Zhang, Y. Hu, and Q. Chen, "Lensless phase microscopy and diffraction tomography with multi-angle and multi-wavelength illuminations using a led matrix," Opt. Express **23**, 14314–14328 (2015).
9. A. K. Gupta and N. K. Nishchal, "A composite method of transport-of-intensity equation for the recovery of broad range of spatial frequencies," J. Opt. **51**, 605–612 (2022).
10. S. D. Grant, K. Richford, H. L. Burdett, D. McKee, and B. R. Patton, "Low-cost, open-access quantitative phase imaging of algal cells using the transport of intensity equation," R. Soc. Open Sci. **7**, 191921 (2020).
11. C. Dorrer and J. D. Zuegel, "Optical testing using the transport-of-intensity equation," Opt. Express **15**, 7165–7175 (2007).
12. Z. Jingshan, R. A. Claus, J. Dauwels, L. Tian, and L. Waller, "Transport of intensity phase imaging by intensity spectrum fitting of exponentially spaced defocus planes," Opt. Express **22**, 10661–10674 (2014).
13. L. Waller, Y. Luo, S. Y. Yang, and G. Barbastathis, "Transport of intensity phase imaging in a volume holographic micro-

scope," Opt. Lett. **35**, 2961–2963 (2010).
14. C. Zuo, Q. Chen, W. Qu, and A. Asundi, "Noninterferometric single-shot quantitative phase microscopy," Opt. Lett. **38**, 3538–3541 (2013).
15. Y. Li, J. Di, C. Ma, J. Zhang, J. Zhong, K. Wang, T. Xi, and J. Zhao, "Quantitative phase microscopy for cellular dynamics based on transport of intensity equation," Opt. Express **26**, 586–593 (2018).
16. A. K. Gupta, R. Mahendra, and N. K. Nishchal, "Single-shot phase imaging based on transport of intensity equation," Opt. Commun. **477**, 126347 (2020).
17. W. Yu, X. Tian, X. He, X. Song, L. Xue, C. Liu, and S. Wang, "Real time quantitative phase microscopy based on single-shot transport of intensity equation (ssTIE) method," Appl. Phys. Lett. **109**, 071112 (2016).
18. X. Zhang, S. Yang, Y. Li, J. Zhang, G. Zheng, Y. Zhang, S. Zhou, and J. Zhu, "Single-shot common-path transport of intensity equation method with Greek-ladder sieves," Opt. Lasers Eng. **126**, 105898 (2020).
19. N. Hai, R. Kumar, and J. Rosen, "Single-shot TIE using polarization multiplexing (STIEP) for quantitative phase imaging," Opt. Lasers Eng. **151**, 106912 (2022).
20. C. Chen, Y.-N. Lu, H. Huang, K. Yan, Z. Jiang, X. He, Y. Kong, C. Liu, F. Liu, L. Xue, and S. Wang, "Phasermic: Phase real-time microscope camera for live cell imaging," Biomed. Opt. Express **12**, 5261–5271 (2021).
21. C. M. Nguyen and H.-S. Kwon, "Common-path off-axis incoherent Fourier holography with a maximum overlapping interference area," Opt. Lett. **44**, 3406–3409 (2019).